Journal of Medicinal Chemistry Article

J. Med. Chem. **2010,** *53,* 4399–4411 **4399**
DOI: 10.1021/jm1002793

Discovery of Imidazo[1,5-*a*]pyrido[3,2-*e*]pyrazines as a New Class of Phosphodiesterase 10A Inhibitors†

Norbert Höfgen,*,‡ Hans Stange,‡ Rudolf Schindler,‡ Hans-Joachim Lankau,‡ Christian Grunwald,‡ Barbara Langen,‡ Ute Egerland,‡ Peter Tremmel,‡ Menelas N. Pangalos,§ Karen L. Marquis,§ Thorsten Hage,‡ Boyd L. Harrison,§ Michael S. Malamas,§ Nicholas J. Brandon,§ and Thomas Kronbach‡

‡*Biotie Therapies GmbH, Meissner Strasse 191, 01445 Radebeul, Germany, and* §*Pfizer Neuroscience Princeton, 865 Ridge Road, Monmouth Junction, New Jersey 08852*

Received March 3, 2010

Novel imidazo[1,5-*a*]pyrido[3,2-*e*]pyrazines have been synthesized and characterized as both potent and selective phosphodiesterase 10A (PDE10A) inhibitors. For in vitro characterization, inhibition of PDE10A mediated cAMP hydrolysis was used and a QSAR model was established to analyze substitution effects. The outcome of this analysis was complemented by the crystal structure of PDE10A in complex with compound **49**. Qualitatively new interactions between inhibitor and binding site were found, contrasting with previously published crystal structures of papaverine-like inhibitors. In accordance with the known antipsychotic potential of PDE10A inhibitors, MK-801 induced stereotypy and hyperactivity in rats were reversed by selected compounds. Thus, a promising compound class has been identified for the treatment of schizophrenia that could circumvent side effects connected with current therapies.

Introduction

Phosphodiesterases (PDEs[a]) are a family of enzymes that inactivate cyclic nucleotides cAMP and cGMP via hydrolyzation.[1] Because cAMP and cGMP are important secondary messengers in the signal cascade of G-protein-coupled receptors, PDEs are involved in a broad spectrum of physiological mechanisms which contribute to the homeostasis of the organism.[2]

In mammals, 11 PDE isoenzyme families have been identified so far,[3] encoded by 21 genes. The PDE families differ in their substrate specificity for cyclic nucleotides, regulatory mechanisms, and sensitivity to inhibitors.[1] Moreover, they are differentially expressed at the tissue, cellular, and subcellular level.[4] These differences result in a diverse array of roles for the PDEs across a range of physiological functions.

PDE10A is a dual substrate PDE, primarily expressed in the brain, specifically in the nucleus accumbens and the caudate putamen. Areas with moderate expression levels include thalamus, hippocampus, frontal cortex, and olfactory tubercle.[5−7] Each of these brain areas is thought to be critical in the pathophysiology of schizophrenia.[8]

The antipsychotic activity of PDE10A inhibitors was first identified using a prototype PDE inhibitor 1-(3,4-dimethoxybenzyl)-6,7-dimethoxyisoquinoline **1** (papaverine, Chart 1), a potent (IC_{50} = 76 nM) and selective PDE10A inhibitor.[9,10]

Chart 1

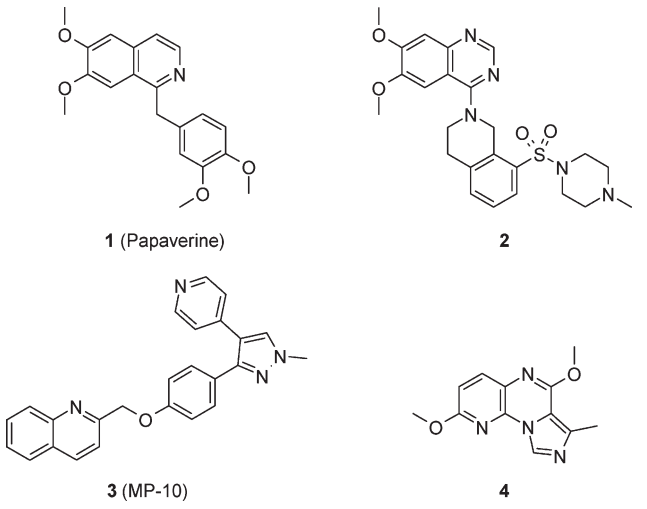

Kostowski et al.[11] showed that papaverine reduces apomorphine-induced stereotypies in a rat model of psychosis and increases haloperidol-induced catalepsy in rats while concurrently reducing brain dopamine concentration. Papaverine also increased striatal extracellular cAMP and cGMP levels[10] but had no effect on cGMP levels in PDE10A KO mice, suggesting that the effects of papaverine were PDE10A-mediated. In addition, papaverine demonstrated efficacy in a broad range of psychosis models including "conditioned avoidance responding" as well as reversal of PCP and D-amphetamine induced hyperactivity. In a separate study, papaverine improved executive function in a rat model,[12] suggesting that the PDE10A mechanism may have a broader therapeutic profile and will provide an approach for treating cognitive deficits of the disease as well as the positive symptoms.

†Coordinates of the PDE10/compound **49** complex have been deposited in the Protein Data Bank. PDB ID is 3LXG.

*To whom correspondence should be addressed. Phone: (+49) 351 40 43 1301. Fax: (+49) 351 40 43 2169. E-mail: norbert.hoefgen@biotie.com.

[a] Abbreviations: cAMP, cyclic adenosine monophosphate; cGMP, cyclic guanine monophosphate; FWA, Free−Wilson analysis; IC_{50}, concentration of inhibitor leading to 50% inhibition; MED, minimal effective dose; PDE, cyclic nucleotide phosphodiesterase; pIC_{50}, $-\log(IC_{50}\,[M])$; (Q)SAR, (quantitative) structure−activity relationship; SEM, standard error of the mean.

Published on Web 05/07/2010

Papaverine was used as starting point for a number of lead optimization programs accompanied by pharmacophore modeling and cocrystallization studies. 6,7-Dimethoxy-4-[8-(4-methyl-piperazine-1-sulfonyl)-3,4-dihydro-1*H*-isoquinolin-2-yl]-quinazoline **2** from Pfizer (Chart 1) was one of the first examples used for X-ray studies of PDE10A complexes.[13] Structure-based drug design permitted identification of a number of high affinity inhibitors of PDE10A. However, lack of isoenzyme selectivity toward PDE3 remains an issue in many cases.

The introduction of biaryl pyrazoles as a new type of PDE10A inhibitors, structurally distinct from papaverine, generated a series of potent PDE10A inhibitors with improved selectivity over other PDEs. Currently, the most advanced example is 2-[4-(1-methyl-4-pyridin-4-yl-1*H*-pyrazol-3-yl)-phenoxymethyl]-quinoline **3** (PF-2545920/MP-10, Chart 1), which is undergoing phase II clinical studies.[14]

Other PDE10A inhibitors, not listed here, have recently been reviewed elsewhere.[15,16]

In the course of our studies to identify isoenzyme selective inhibitors of PDE10A, we discovered the imidazo[1,5-*a*]-pyrido[3,2-*e*]pyrazines as a new compound class. Random screening yielded first experimental indications as to the suitability of these compounds. On the basis of this screen, compound **4** (Chart 1) was selected for structure optimization.

Results and Discussion

Chemistry. The synthetic procedures of imidazo[1,5-*a*]-pyrido[3,2-*e*]pyrazines (Table 1) are outlined in Schemes 1−7. Key starting points are imidazo[1,5-*a*]pyrido[3,2-*e*]-pyrazinones (**I**), synthesized according to the method of Norris et al.[17] Treatment of **I** with $POCl_3$ produced the corresponding 4-chloro-imidazo[1,5-*a*]pyrido[3,2-*e*]pyrazines (**II**). The chlorine atom can be replaced via classical nucleophilic substitution reactions in the presence of potassium hydroxide (Scheme1). Nucleophiles used here were alcohols for synthesis of **4**−**14**, mercaptanes for derivatives **15**−**18**, and amines for preparation of **22**−**24**. Under similar conditions, potassium cyanide was used to prepare nitriles **25**−**27**.

Stepwise oxidation of 4-methylmercapto-imidazo[1,5-*a*]-pyrido[3,2-*e*]pyrazines (**III**) with 3-chloroperoxybenzoic acid produced the corresponding sulfines and sulfones **19**−**21** (Scheme 2). Individual products were separated by preparative HPLC.

Treatment of **II** with ammonia or methylamine formed 4-amino-imidazo[1,5-*a*]pyrido[3,2-*e*]pyrazines (**IV**), which upon reaction with anhydrides or carboxylic acid chlorides produced carboxylic acid amides **28**−**30** (Scheme 3). To investigate the role of the remaining hydrogen at the amide group, a second acylation was carried out to synthesize compound **33**.

4-Alkoxycarbonylamino-imidazo[1,5-*a*]pyrido[3,2-*e*]pyrazines **31**, **32**, and **34** were prepared using chloroformic acid esters for acylation. Ureas **35**−**37** were synthesized by reacting **IV** with carbonyldiimidazole and amines or ammonia.

For comparison with carboxylic acid amides, a series of corresponding sulfonamides **38**−**45** were prepared from **IV** by treatment with sulfonic acid chlorides or anhydrides in an aprotic solvent (Scheme 4). Depending on the structure of the 4-amino-imidazo[1,5-*a*]pyrido[3,2-*e*]pyrazine and the amount of sulfonic acid derivative, either one or two (**43**) sulfonations were obtained.

Hydrogenation of **II** displaced the chlorine atom exemplified here with compound **46**. 4-Alkyl-imidazo[1,5-*a*]pyrido-[3,2-*e*]pyrazines **47**−**59** and **62** were synthesized by the reaction of **II** with Grignard reagents (Scheme 5).

For synthesis of 4-trifluoromethyl-imidazo[1,5-*a*]pyrido-[3,2-*e*]pyrazine **61**, this approach was modified by first replacing chlorine by iodine and subsequently treating with trifluoromethyl-tris-methylsilane (Scheme 6).

An alternative synthetic route was used for preparation of 4-alkyl-imidazo[1,5-*a*]pyrido[3,2-*e*]pyrazines **60**, **63**−**64** (Scheme 7). 4-Amino-2-(4-methyl-2-propyl-imidazolyl)-6-methoxy-pyridine was treated with carboxylic acid anhydrides to form the corresponding amides, which were cyclocondensed at higher temperatures.

Inhibition of PDE10 Activity: SAR and QSAR. Inhibitory potencies of our compounds were tested using in vitro inhibition of human recombinant PDE10A catalyzed cAMP hydrolysis. The results are compiled in Table 1.

The impact of R^1 on target affinity was investigated in a number of subseries of derivatives. The replacement of the hydrogen in compound **4** with an aliphatic chain yielded a significant improvement in affinity (compounds **5**, **6**, and **8**). The *n*-propyl group seems to be the optimal, confirmed with compounds including **11**, **18**, **25**, **39**, and **49**. Similar groups like isobutyl and cyclohexyl are also well tolerated. In contrast, phenyl-substituted chains, e.g. phenylethyl (compound **59**), may be too large at this position, resulting in a slight drop of affinity. R^2 was identified to be a critical position for good affinity. Here only small groups (hydrogen, methyl) can be used. A large variety of substituents was investigated for R^3. Again, small substituents are preferred. Hydrogen (compound **46**), cyano (compounds **25** to **27**), and methyl groups were frequently used to get highly affine derivatives. Among the larger substituents generally reducing target affinity, the methylsulfonylamino group seems to be an exception (compound **39**). Finally, only a narrow range of substituents was tested at position R^4. No major effects on the IC_{50} values were found.

Our initial SAR findings were complemented by a QSAR study to obtain a comprehensive overview of relationships between substituent patterns and biological activity and to differentiate between significant and nonsignificant effects. A Free−Wilson analysis[18] (FWA) as modified by Fujita and Ban[19] was applied. The most frequent R groups were used as standards resulting in a structure that is equal to **49**. Two significant models M1 and M2 were derived. M1: $n = 61$, $r = 0.990$, $s = 0.242$, $F = 13.13$, $p < 0.001$; M2: $n = 27$, $r = 0.979$, $s = 0.242$, $F = 22.83$, $p < 0.001$. M1 is based on all available compounds. For M2, only the subset of compounds with nonunique substituents was included, i.e., with substituents that were used at a specific position in two or more compounds. Model M2 excludes known statistical problems associated with unique substituents.[20] However, M1 may give hints as to which unique substituents may potentially be advantageous. Results of the FWA are compiled in Table 2. Listed coefficients are numerical contributions of the standard-substituted compound and the different substituents to the $-\log(IC_{50})$ value. Positive and negative coefficients indicate an increase in or decrease of inhibition, respectively, compared to standard substitution. Numerical results are presented in detail in the Supporting Information.

Starting from the global result of the FWA, the excellent correlation coefficients indicate that assumptions underlying this QSAR method are met with regard to derivatives with nonunique substituents: There is no indication of

Table 1. Substituent Pattern and Measured Inhibition of PDE10A Activity

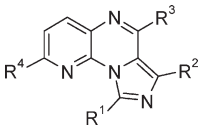

compd	R^1	R^2	R^3	R^4	IC_{50}/INH[a]	SEM[b]
4	H	CH_3	OCH_3	OCH_3	2270	196
5	CH_3	CH_3	OCH_3	OCH_3	270	17.2
6	C_2H_5	CH_3	OCH_3	OCH_3	63.0	3.38
7	C_3H_7	H	OCH_3	OCH_3	92.2	9.44
8	C_3H_7	CH_3	OCH_3	OCH_3	24.8	2.98
9	C_2H_5	CH_3	OC_3H_7	OCH_3	149	17.1
10	C_2H_5	CH_3	$OCH(CH_3)_2$	OCH_3	731	54.1
11	C_3H_7	CH_3	$OCH(CH_3)_2$	OCH_3	391	11.2
12	C_2H_5	CH_3	cyclopentyloxy	OCH_3	25.4%	0.96%
13	C_3H_7	CH_3	$OC_2H_4C_6H_5$	OCH_3	383	31.7
14	C_3H_7	CH_3	$OC_3H_6C_6H_5$	OCH_3	962	125
15	H	CH_3	SCH_3	OCH_3	21.0%	4.31%
16	CH_3	CH_3	SCH_3	OCH_3	2390	288
17	C_2H_5	CH_3	SCH_3	OCH_3	617	51.5
18	C_3H_7	CH_3	SCH_3	OCH_3	209	26.8
19	C_2H_5	CH_3	$S(=O)CH_3$	OCH_3	284	27.3
20	C_3H_7	CH_3	$S(=O)CH_3$	OCH_3	89.6	2.75
21	C_3H_7	CH_3	$S(=O)_2CH_3$	OCH_3	23.3	1.43
22	C_2H_5	CH_3	$NHCH_3$	OCH_3	482	59.8
23	C_3H_7	CH_3	$NHCH_3$	OCH_3	246	34.6
24	C_3H_7	CH_3	$N(CH_3)_2$	OCH_3	146	16.7
25	C_3H_7	CH_3	CN	OCH_3	10.9	1.6
26	C_2H_5	CH_3	CN	OCH_3	36.4	5.3
27	cyclohexyl	CH_3	CN	OCH_3	9.62	1.41
28	C_2H_5	CH_3	$NHC(=O)CH_3$	OCH_3	175	39
29	C_3H_7	CH_3	$NHC(=O)CH_3$	OCH_3	472	61.4
30	C_3H_7	CH_3	$NHC(=O)C_2H_5$	OCH_3	1050	169
31	C_3H_7	CH_3	$NHC(=O)OCH_3$	OCH_3	22.9	1.97
32	C_3H_7	CH_3	$NHC(=O)OC_2H_5$	OCH_3	206	20.5
33	C_3H_7	CH_3	$N(C(=O)OCH_3)_2$	OCH_3	81.5	8.21
34	C_3H_7	CH_3	$N(CH_3)C(=O)OCH_3$	OCH_3	486	54.2
35	C_3H_7	CH_3	$NHC(=O)NH_2$	OCH_3	55.4	7.82
36	C_3H_7	CH_3	$NHC(=O)NHCH_3$	OCH_3	535	47.3
37	C_3H_7	CH_3	$NHC(=O)NHCH(CH_3)_2$	OCH_3	381	49.1
38	C_2H_5	CH_3	$NHS(=O)_2CH_3$	OCH_3	64.7	3.96
39	C_3H_7	CH_3	$NHS(=O)_2CH_3$	OCH_3	7.16	0.74
40	C_3H_7	CH_3	$NHS(=O)_2C_2H_5$	OCH_3	39.2	2.01
41	C_3H_7	CH_3	$NHS(=O)_2C_3H_7$	OCH_3	617	10.7
42	C_3H_7	CH_3	$NHS(=O)_2CH(CH_3)_2$	OCH_3	132	15.6
43	C_3H_7	CH_3	$N(S(=O)_2CH_3)_2$	OCH_3	15.3	1.07
44	C_3H_7	CH_3	$NHS(=O)_2CF_3$	OCH_3	53.4	6.77
45	C_3H_7	CH_3	$N(CH_3)S(=O)_2CH_3$	OCH_3	1195	89
46	C_3H_7	CH_3	H	OCH_3	33.9	4.69
47	CH_3	CH_3	CH_3	OCH_3	81.2	3.46
48	C_2H_5	CH_3	CH_3	OCH_3	15.7	0.44
49	C_3H_7	CH_3	CH_3	OCH_3	7.28	0.6
50	C_3H_7	H	CH_3	OCH_3	25.1	1.91
51	C_3H_7	CH_3	CH_3	H	32.5	3.16
52	C_3H_7	CH_3	CH_3	CH_3	8.32	0.47
53	C_3H_7	CH_3	CH_3	$OCHF_2$	13.2	0.82
54	C_5H_{11}	CH_3	CH_3	OCH_3	51.3	2.28
55	C_6H_{13}	CH_3	CH_3	OCH_3	223	26.8
56	cyclohexyl	CH_3	CH_3	OCH_3	2.84	0.355
57	$CH_2CH(CH_3)_2$	CH_3	CH_3	OCH_3	1.43	0.23
58	$CH_2C_6H_5$	CH_3	CH_3	OCH_3	21.4	2.17
59	$C_2H_4C_6H_5$	CH_3	CH_3	OCH_3	116	13.1
60	C_3H_7	CH_3	CHF_2	OCH_3	7.33	0.7
61	C_3H_7	CH_3	CF_3	OCH_3	45.8	2.12
62	C_3H_7	CH_3	C_2H_5	OCH_3	12.4	1.15
63	C_3H_7	$C(=O)OCH_3$	CH_3	OCH_3	285	35.7
64	C_3H_7	$C(=O)OC_2H_5$	CH_3	OCH_3	326	5.7
1					56.9	4.4
3					1.34	0.19

[a] Means of IC_{50} [nmol/L] or, in case of **12** and **15**, percent inhibition at a concentration of 1000 nM; $n = 4$. [b] Standard error of the mean

Scheme 1

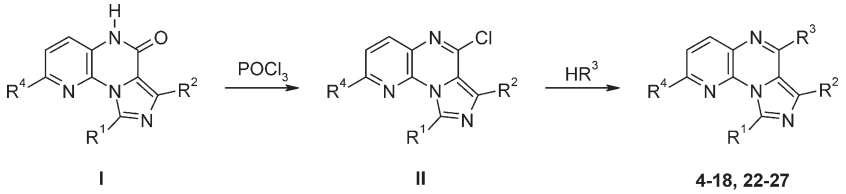

Scheme 2

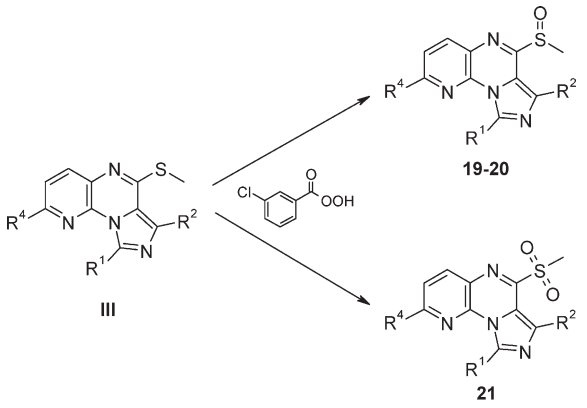

interactions between the four substituents, and the implicitly used simple alignment of the three-ring systems appears to be correct. From the alignment, we conclude that at least this subset of compounds will have a similar binding position compared to **49** for which the PDE10 cocrystal structure was solved. Docking calculations were used to further check this assumption (see below). Regarding the four substituents, standard substitution is generally favorable with regard to IC_{50}. At position R^1, inhibition may be enhanced by use of isobutyl (unique substituent) instead of propyl. Smaller as well as the majority of larger substituents decrease inhibition but cyclohexyl and benzyl do not change the IC_{50} significantly, indicating a voluminous subpocket. Only a small number of substituents were used at position R^2. Among these, the standard methyl is optimal in comparison to both smaller (hydrogen) and larger (ester) groups. A large spectrum of substituents was applied at position R^3. No substituents offering significant improvement on the standard methyl were found. Smaller (hydrogen) and most larger and polar substituents decrease the inhibitory potential. However, two comparatively large sulfonamide groups do not change IC_{50} values significantly. It can thus be hypothesized that there is, in this position, space for bulkier groups and specific interactions such as hydrogen bonding. At position R^4, only four groups were tested. No significant differences were found between polar methoxy and difluoromethoxy

Scheme 4

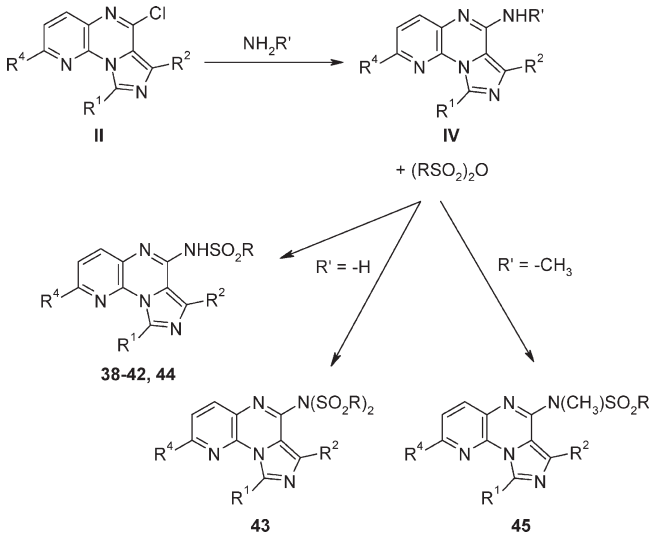

Scheme 3

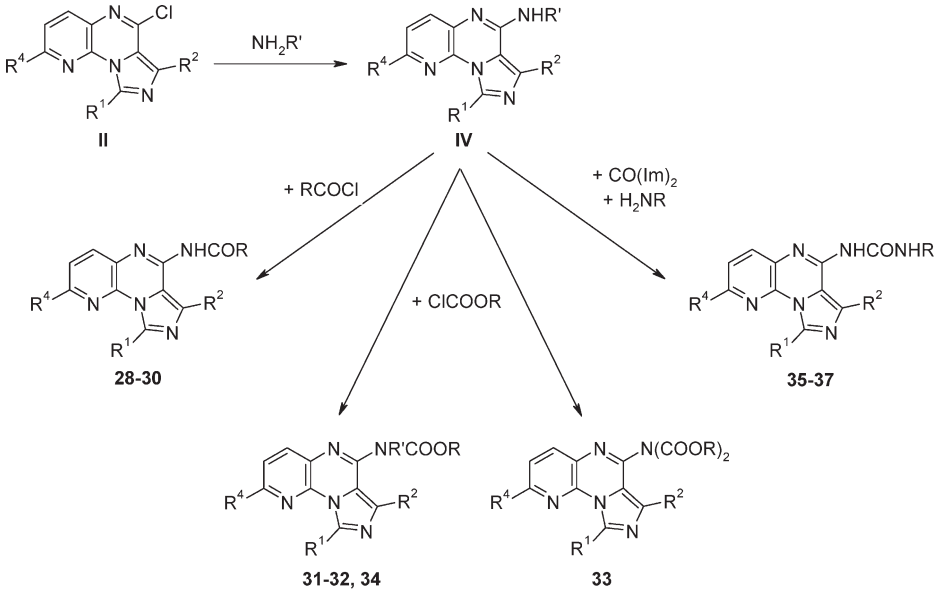

Scheme 5

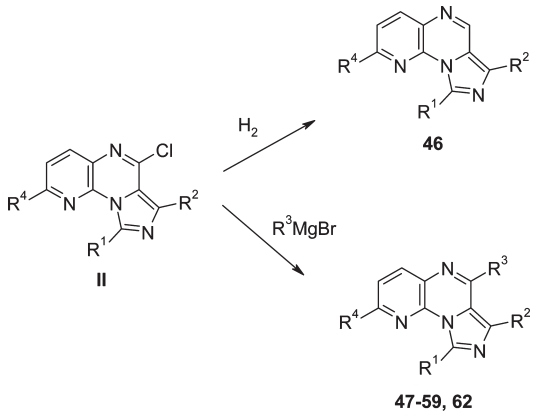

Scheme 6

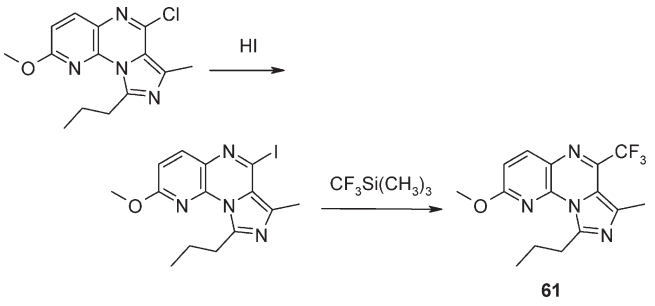

Scheme 7

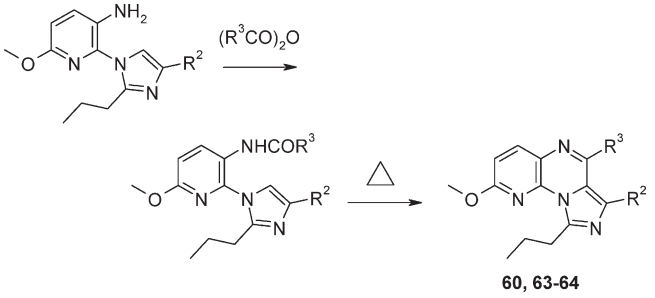

groups and nonpolar methyl. The small hydrogen atom however decreases inhibitory potency.

X-ray. Crystal structure determination of the potent compound **49** in complex with PDE10A (rat) was used to complement data obtained from SAR studies regarding binding posture and key interactions of the invariant core structure and binding site residues. The structure of a papaverine-like inhibitor in complex with PDE10A is known[21] and displays some similarities with inhibitors of other PDE's, e.g. rolipram at PDE4D.[22] Recently, the structure of PDE10A in complex with papaverine was published.[23] In contrast to this data, qualitatively new interactions were to be expected with our compounds due to the lack of a dimethoxy moiety and the new core structure.

Binding interactions of compound **49** are summarized schematically in Figure 2, and the binding pocket is depicted in Figure 3. **49** interacts with Gln716 via a hydrogen bond to the pyrazine nitrogen. This glutamine residue is conserved in all PDE isoforms and known to play a crucial role in binding natural PDE substrates cGMP and cAMP.[24,25] It is also involved in hydrogen bonding interactions with most known PDE inhibitors. Additional water-mediated hydrogen bonds between the imidazole nitrogen and residues Tyr514 and Asp664 further anchor this inhibitor within the binding site. This hydrogen bond network is not known from other PDE10A inhibitors.[26] The binding pose is further stabilized

Table 2. Free−Wilson Analysis Results: Substituent Coefficients

Pos.	substituent	coefficient C^a
CS	standard-substituted compound	8.168[b]
R^1	$CH_2CH(CH_3)_2$	(0.677)[c]
	cyclohexyl	ns[d]
	C_3H_7[e]	**0**
	C_2H_5	−0.369
	$CH_2C_6H_5$	(ns)
	C_5H_{11}	(−0.878)
	CH_3	−1.047
	$C_2H_4C_6H_5$	(−1.232)
	C_6H_{13}	(−1.516)
	H	−1.593
R^2	**CH_3**	**0**
	H	−0.526
	$C(=O)OCH_3$	(−1.623)
	$C(=O)OC_2H_5$	(−1.681)
R^3	**CH_3**	**0**
	CHF_2	(ns)
	C_2H_5	(ns)
	$NHS(=O)_2CH_3$	ns
	CN	−0.332
	$N(S(=O)_2CH_3)_2$	(ns)
	$NHC(=O)OCH_3$	(−0.528)
	$S(=O)_2CH_3$	(−0.535)
	OCH_3	−0.65
	H	(−0.698)
	$NHS(=O)_2C_2H_5$	(−0.761)
	CF_3	(−0.829)
	$NHS(=O)_2CF_3$	(−0.896)
	$NHC(=O)NH_2$	(−0.912)
	OC_3H_7	(−0.972)
	$N(C(=O)OCH_3)_2$	(−1.079)
	$S(=O)CH_3$	−1.186
	$NHS(=O)_2CH(CH_3)_2$	(−1.289)
	$N(CH_3)_2$	(−1.332)
	SCH_3	−1.432
	$NHC(=O)CH_3$	−1.442
	$NHC(=O)OC_2H_5$	(−1.482)
	$NHCH_3$	−1.521
	$OCH(CH_3)_2$	−1.712
	$NHC(=O)NHCH(CH_3)_2$	(−1.749)
	$OC_2H_4C_6H_5$	(−1.751)
	$N(CH_3)C(=O)OCH_3$	(−1.855)
	$NHC(=O)NHCH_3$	(−1.896)
	$NHS(=O)_2C_3H_7$	(−1.958)
	$OC_3H_6C_6H_5$	(−2.151)
	$NHC(=O)C_2H_5$	(−2.189)
	$N(CH_3)S(=O)_2CH_3$	(−2.245)
	cyclopentyloxy	(−2.267)
R^4	**OCH_3**	**0**
	CH_3	(ns)
	$OCHF_2$	(ns)
	H	(−0.68)

[a] Coefficients C from multiple linear regression analysis. $pIC_{50} = -\log(IC_{50}) = C_{CS} + C_{R1} + C_{R2} + C_{R3} + C_{R4}$. [b] Related coefficients of models M1 and M2 are identical. [c] Results for unique substituents are stated in parentheses. [d] ns: not significantly different from zero: $p > 0.1$. [e] Standard substituent bold.

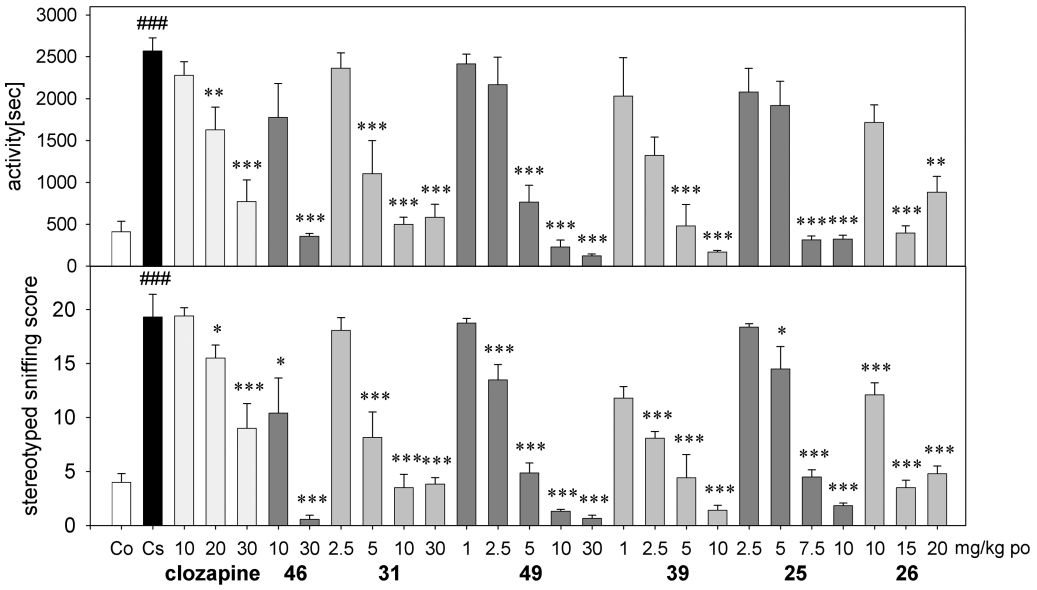

Figure 1. Effect of PDE10 inhibitors on MK-801 induced hyperactivity and stereotyped sniffing in female rats. Data are shown as mean ± SEM. Significantly different from MK-801 stimulated control (Cs): * $p < 0.05$, ** $p < 0.01$, *** $p < 0.001$. Significantly different from saline control (Co): ### $p < 0.001$.

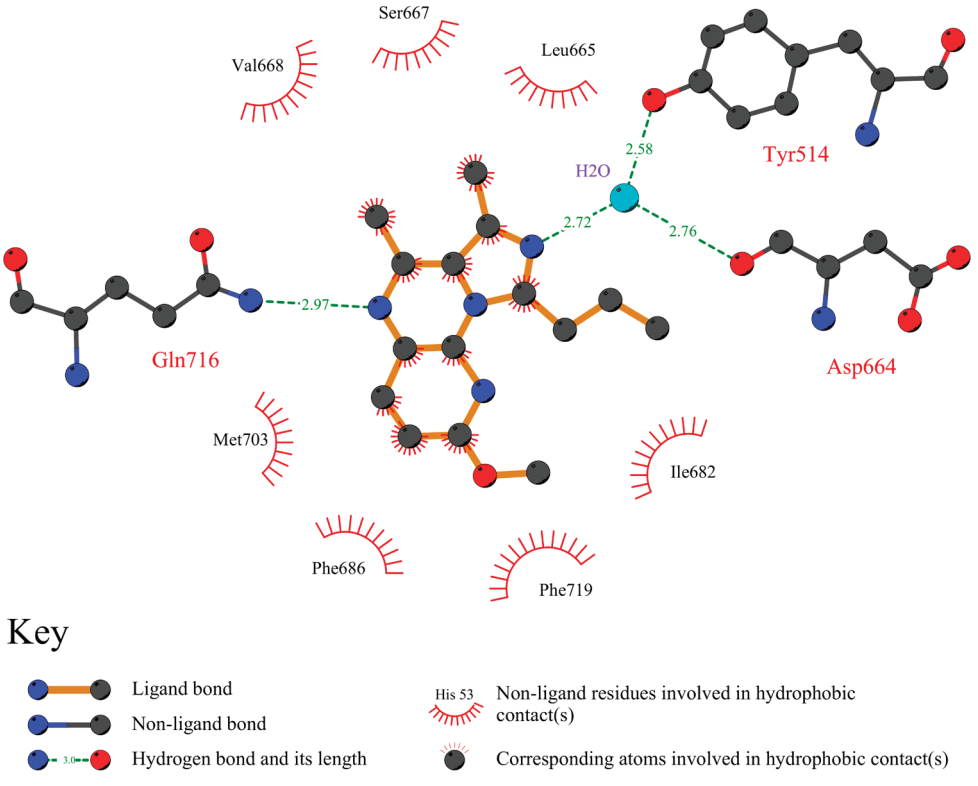

Figure 2. Ligplot[38] representation of hydrophobic and hydrogen bond interactions of compound **49** and the amino acid residues involved in the PDE10 binding pocket.

by π-stacking of the fused ring system with Phe719 and hydrophobic contacts with Leu665, Ser667, Val668, Ile682, Phe686, and Met703. Phe719, Phe686, and Ile682 form a cleft known as a "hydrophobic clamp".[27] On the basis of the crystal structure, some aspects of the experimentally observed SAR can be rationalized. At positions R^1 (propyl) and R^4 (methoxy), no interactions were detected (Figure 2), indicating room for larger substituents. The oxygen of R^4 is not involved in polar interactions or hydrogen bonding. Methyl at position R^2 has the optimal size to occupy a small subpocket. The R^2 substituent is involved in hydrophobic interactions with a couple of amino acid residues. As we found in our SAR studies, there is no space to accommodate larger groups. In contrast, a methyl group at the R^3 position points toward a rather large subpocket. There are hydrophobic contacts with Ile682 and Val668, but there is space for bulkier groups which could be involved in additional interactions. The methylsulfonamide substituent of **39** is one such example.

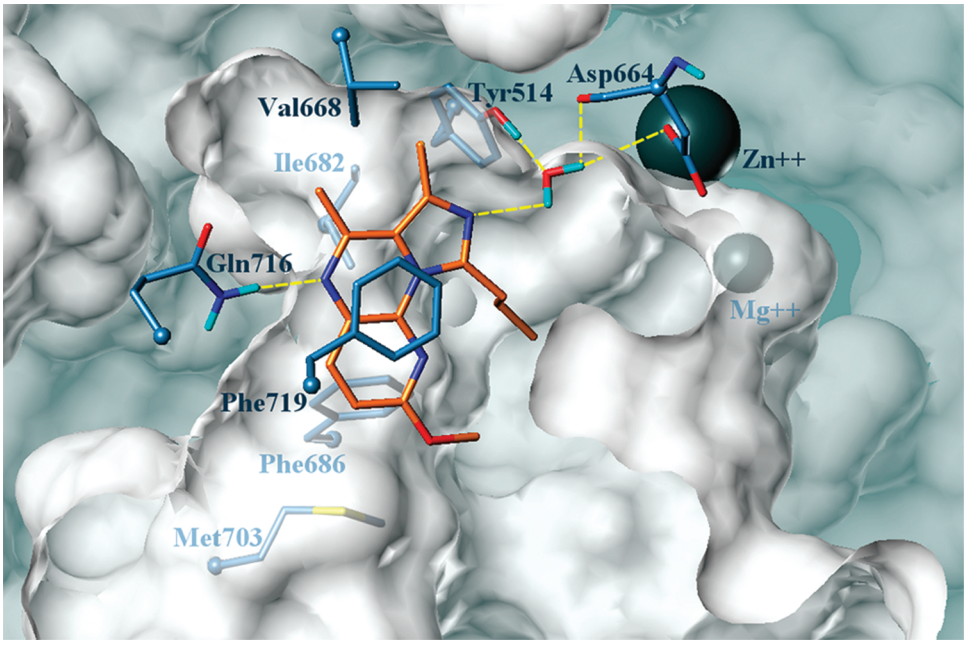

Figure 3. Co-crystal structure of PDE10 and **49** (orange C atoms): depiction of the shape of the binding pocket (clipped in *z* direction), key amino acids (blue−gray C atoms), metal ions (spheres), and a water involved in binding. H bonds are symbolized by yellow broken lines.

Table 3. Reversal of MK-801 Induced Hyperactivity and Stereotyped Sniffing

compd	MED[a] hyperact (mg/kg po)	*F* hyperact[b]	MED[a] sniffing (mg/kg po)	*F* sniffing[b]	IC_{50} (nM)[c]
25	7.5	34.813	5	47.893	10.9
26	15	14.764	10	58.876	36.4
31	5	20.180	5	43.586	22.9
39	5	13.684	2.5	29.536	7.16
46	30	17.360	10	23.693	33.9
49	5	29.580	2.5	94.475	7.28
clozapine	20	16.533	20	16.279	n.i.[d]

[a] Minimal effective dose that significantly reduced MK-801-induced hyperactivity or stereotyped sniffing, respectively ($p < 0.05$). [b] $p < 0.001$, $n = 6$. [c] Inhibition of PDE10 activity from Table 2. [d] ni: no inhibition at PDE10.

To test our initial hypothesis of a similar binding mode of our compounds, **4**−**64** were docked into the crystal structure. It was found that most derivatives can adopt a binding position like **49**, even those with rather big R^3 substituents (sulfonamides, ureas, urethanes). However, the extended R^3 substituents of **12**, **13**, **14**, and **33** on the one hand and R^2 ester groups of **63** and **64** on the other hand do not seem to fit into the respective subpockets—only alternative binding poses were calculated. Interestingly, there is no total loss of inhibitory potency despite a likely changed binding mode. Thus, these derivatives might be used as starting points for new PDE10 inhibitors. Because the four R^3 and two R^2 substituents causing potentially changed binding poses are unique in the present set of derivatives, SAR (either qualitative or QSAR like FWA) did not allow determination if reduced inhibition was due to unfavorable local interaction or changed binding mode. Recalculation of FWA model M1 without **12**, **13**, **14**, **33**, **63**, and **64** yielded identical regression coefficients for all other substituents and nearly unchanged statistics.

Pharmacology. A representative subset of six high affinity PDE10A inhibitors was selected for investigation of the antipsychotic potential of imidazo[1,5-a]pyrido[3,2-e]pyrazines in vivo. To enable the characterization of the antipsychotic activity, we utilized a MK-801 induced hyperactivity reversal model.[28] MK-801 (0.1 mg/kg ip) significantly increased horizontal activity (*t* test: $p < 0.001$) and induced stereotyped sniffing (*t* test: $p < 0.001$) in female rats. These behaviors were reversed significantly by 8-chloro-11-(4-methyl-1-piperazinyl)-5*H*-dibenzo(*b*,*e*)(1,4)diazepine (clozapine), an atypical antipsychotic.[29] The selected PDE10A inhibitors also reversed hyperactivity and stereotyped sniffing in a dose dependent and significant manner. Results are shown in Table 3 and Figure 1.

Table 4. Selectivity of **39** and **49** towards PDE Isoforms

	IC_{50}[a] [nM]	
PDE	**39**	**49**
1B	> 1000	> 5000
2A	~1000	239 (25)
3A	1260 (125)	3700 (491)
4A	> 1000	~5000
5A	561 (77)	919 (81)
6	> 1000	> 5000
7B	> 1000	3100 (491)
8A	> 1000	> 5000
9A	> 1000	> 5000
10A	7.16 (0.74)	7.28 (0.60)
11A	68.6 (3.9)	779 (107)

[a] SEM of IC_{50} data stated in parentheses if IC_{50} values could be determined. Otherwise, IC_{50} values are related to the maximum concentration used in the screen.

The minimal effective dose (MED) of clozapine for both end points is 20 mg/kg; the MEDs of the novel PDE10A inhibitors

are, with one exception, below this value (Table 3). Further, a qualitative correlation can be seen between MEDs and PDE10 inhibition data. Among the six compounds studied, **39** and **49** are most effective regarding both enzyme inhibition and reversal of MK-801 induced behavioral symptoms. Both compounds were characterized regarding their selectivity profiles. They were found to be highly specific PDE10A inhibitors with selectivities >100 to most of the isoenzymes: Table 4.

Conclusions

A series of novel imidazo[1,5-*a*]pyrido[3,2-*e*]pyrazines has been identified. These compounds were characterized to be potent and selective PDE10A inhibitors structurally distinct from inhibitor families published to date. Structural optimization was supported by a QSAR model established to analyze substitution effects. The optimal combination of substituents was realized with compound **49**. The outcome of this analysis was complemented by the crystal structure of PDE10A in complex with compound **49**. Qualitatively distinct interactions between inhibitor and binding site were found contrasting with previously published crystal structures of papaverine-like inhibitors. In addition to the common hydrogen bond to Gln716, a water mediated interaction between the imidazole nitrogen and Tyr514 and Asp664 was detected. This hydrogen bond network was not known from other types of PDE10A inhibitors. In accordance with the known antipsychotic potential of PDE10A inhibitors, MK-801 induced stereotypies and hyperactivity in rats were reversed by selected compounds. The most effective derivatives are compounds **39** and **49**, with MED's of 2.5 and 5 mg/kg po, respectively. Compound **49** is favorable with regard to its selectivity toward all other PDE's. Thus, a promising compound class for the treatment of schizophrenia has been found.

Experimental Section

Chemistry. Column chromatography was performed on silica gel eluting with 5% MeOH in CH_2Cl_2. Melting points were determined on a Boetius melting point apparatus PHMK 05 and are uncorrected. All substances were analyzed with an Agilent 1100 series HPLC/MSD system. Purities were ascertained using the area percentage method on the UV trace recorded at a wavelength of 254 nm and found to be ≥95%. Proton (^{1}H NMR) and carbon (^{13}C NMR) nuclear magnetic resonance spectra were recorded on a Bruker ARX 300 NMR spectrometer. Chemical shifts (δ) are in parts per million (ppm) relative to $Si(CH_3)_4$, and coupling constants (J) are in hertz. The NMR solvent used was either $CDCl_3$ or DMSO. Analytical and spectroscopic data are listed here only for key compounds. A comprehensive list including all compounds can be found in Supporting Information.

Key Intermediates. The synthesis of the used imidazo[1,5-*a*]-pyrido[3,2-*e*]pyrazinones **I** is described by Norris et al.[17] The synthesis of the used 4-chloro-imidazo[1,5-*a*]pyrido[3,2-*e*]pyrazines **II** is described by Chen et al.[30]

Synthesis of 4-Alkoxy-imidazo[1,5-*a*]pyrido[3,2-*e*]pyrazines 4−14. General Procedure. First, 5 mmol of 4-chloro-imidazo-[1,5-*a*]pyrido[3,2-*e*]pyrazine were dissolved in a mixture of 15 mL of dichloromethane and 15 mL of the corresponding alcohol, then 1 g of solid KOH was added. The reaction mixture was heated up to reflux for 7 h. At room temperature, 30 mL of water were added. The organic layer was separated. The aqueous layer was extracted with 20 mL of dichloromethane. The unified organic layers were washed with two times 20 mL of water. The solvent was removed completely. The residue was purified by column chromatography.

4,8-Dimethoxy-3-methyl-imidazo[1,5-*a*]pyrido[3,2-*e*]pyrazine (4). Yield 72%; mp 152−154 °C; $C_{12}H_{12}N_4O_2$; MW 244.25. ^{1}H NMR (300 MHz, $CDCL_3$) δ 8.55 (s, 1 H), 7.73 (d, J = 9 Hz, 1 H), 6.71 (d, J = 9 Hz, 1 H), 4.03 (s, 3 H), 3.95 (s, 3 H), 2.60 (s, 3 H). ^{13}C NMR (300 MHz, $CDCL_3$) δ 160.72, 154.61, 137.96, 136.66, 133.95, 128.57, 124.12, 115.36, 109.97, 53.90, 53.39, 14.33.

4,8-Dimethoxy-1,3-dimethyl-imidazo[1,5-*a*]pyrido[3,2-*e*]pyrazine (5). See Supporting Information for details.

4,8-Dimethoxy-1-ethyl-3-methyl-imidazo[1,5-*a*]pyrido[3,2-*e*]-pyrazine (6). See Supporting Information for details.

4,8-Dimethoxy-1-propyl-imidazo[1,5-*a*]pyrido[3,2-*e*]pyrazine (7). See Supporting Information for details.

4,8-Dimethoxy-3-methyl-1-propyl-imidazo[1,5-*a*]pyrido[3,2-*e*]-pyrazine (8). See Supporting Information for details.

1-Ethyl-8-methoxy-3-methyl-4-propyloxy-imidazo[1,5-*a*]pyrido-[3,2-*e*]pyrazine (9). See Supporting Information for details.

1-Ethyl-8-methoxy-3-methyl-4-isopropyloxy-imidazo[1,5-*a*]-pyrido[3,2-*e*]pyrazine (10). See Supporting Information for details.

4-Isopropyloxy-8-methoxy-3-methyl-1-propyl-imidazo[1,5-*a*]-pyrido[3,2-*e*]pyrazine (11). See Supporting Information for details.

1-Ethyl-8-methoxy-3-methyl-4-cyclopentyloxy-imidazo[1,5-*a*]-pyrido[3,2-*e*]pyrazine (12). See Supporting Information for details.

8-Methoxy-3-methyl-4-phenethyloxy-1-propyl-imidazo[1,5-*a*]-pyrido[3,2-*e*]pyrazine (13). See Supporting Information for details.

8-Methoxy-3-methyl-4-(3-phenyl-propoxy)-1-propyl-imidazo-[1,5-*a*]pyrido[3,2-*e*]pyrazine (14). See Supporting Information for details.

Synthesis of 4-Methylsulfanyl-imidazo[1,5-*a*]pyrido[3,2-*e*]pyrazines 15−18. General Procedure. First, 5 mmol of 4-chloro-imidazo[1,5-a]pyrido[3,2-e]pyrazine were dissolved in 25 mL of *N*,*N*-dimethylformamide, then 20 mmol of sodium thiomethylate were added. The mixture was heated up to 60 °C for 4 h. The solvent was removed, and the residue was treated with 20 mL of water and 20 mL of dichloromethane. The organic layer was separated. The aqueous layer was extracted with 20 mL of dichloromethane. The unified organic layers were washed with two times 20 mL of water. The solvent was removed completely. The residue was purified by column chromatography.

8-Methoxy-3-methyl-4-methylsulfanyl-imidazo[1,5-*a*]pyrido-[3,2-*e*]pyrazine (15). Yield 69%; mp 185−187 °C; $C_{12}H_{12}N_4OS$; MW 260.32. ^{1}H NMR (300 MHz, $CDCL_3$) δ 8.60 (s, 1 H), 7.86 (d, J = 9 Hz, 1 H), 6.75 (d, J = 9 Hz, 1 H), 3.99 (s, 3 H), 2.74 (s, 3 H), 2.62 (s, 3 H). ^{13}C NMR (300 MHz, $CDCL_3$) δ 160.99, 152.92, 138.47, 136.26, 134.11, 127.71, 125.18, 121.15, 110.32, 54.08, 15.75, 12.11.

8-Methoxy-1,3-dimethyl-4-methylsulfanyl-imidazo[1,5-*a*]pyrido-[3,2-*e*]pyrazine (16). See Supporting Information for details.

1-Ethyl-8-methoxy-3-methyl-4-methylsulfanyl-imidazo[1,5-*a*]-pyrido[3,2-*e*]pyrazine (17). See Supporting Information for details.

8-Methoxy-3-methyl-4-methylsulfanyl-1-propyl-imidazo[1,5-*a*]-pyrido[3,2-*e*]pyrazine (18). See Supporting Information for details.

Synthesis of 4-Methylsulfinyl-imidazo[1,5-*a*]pyrido[3,2-*e*]-pyrazines 19−20. General Procedure. First, 2 mmol of 4-methylsulfanyl-imidazo[1,5-*a*]pyrido[3,2-*e*]pyrazine were dissolved in 40 mL of dichloromethane. At 0−5 °C, about 0.8 g of 3-chloroperoxybenzoic acid were added in small portions. The mixture was stirred for 2 h at 5 °C. At room temperature, the reaction solution was washed first with 2 × 30 mL saturated $NaHCO_3$ solution and then with 2 × 30 mL water. The solvent was removed from the isolated organic layer. The residue was purified by column chromatography.

1-Ethyl-8-methoxy-3-methyl-4-methylsulfinyl-imidazo[1,5-*a*]-pyrido[3,2-*e*]pyrazine (19). Yield 67%; mp 189−192 °C; $C_{14}H_{16}N_4O_2S$; MW 304.37. ^{1}H NMR (300 MHz, $CDCL_3$) 8.23 (d, J = 9 Hz, 1 H), 6.89 (d, J = 9 Hz, 1 H), 4.05 (s, 3 H), 3.66 (q, J =

7 Hz, 2 H), 2.94 (s, 3 H), 2.72 (s, 3 H), 1.45 (t, J = 7 Hz, 3 H). ^{13}C NMR (300 MHz, $CDCL_3$) δ 162.64, 156.66, 147.80, 140.63, 137.67, 134.88, 125.24, 120.11, 110.54, 54.42, 39.13, 24.32, 16.28, 13.20.

8-Methoxy-3-methyl-4-methylsulfinyl-1-propyl-imidazo[1,5-*a*]-pyrido[3,2-*e*]pyrazine (20). See Supporting Information for details.

8-Methoxy-3-methyl-4-methylsulfonyl-1-propyl-imidazo[1,5-*a*]-pyrido[3,2-*e*]pyrazine (21). First, 2 mmol of 8-methoxy-4-methylsulfanyl-1-propyl-imidazo[1,5-*a*]pyrido[3,2-*e*]pyrazine (**18**) were dissolved in 40 mL of dichloromethane. At 0−5 °C, about 1.58 g of 3-chloroperoxybenzoic acid were added in small portions. The mixture was stirred for 2 h at 25 °C. At room temperature, the reaction solution was washed first with 2 × 30 mL of saturated $NaHCO_3$ solution and then with 2 × 30 mL of water. The solvent was removed from the isolated organic layer. The residue was purified by column chromatography.

Yield 59%; mp 43−46 °C; $C_{15}H_{18}N_4O_3S$; MW 334.4. ^{1}H NMR (300 MHz, $CDCL_3$) 7.95 (d, J = 9 Hz, 1 H), 6.83 (d, J = 9 Hz, 1 H), 4.02 (s, 3 H), 3.57 (t, J = 8 Hz, 2 H), 3.40 (s, 3 H), 2.79 (s, 3 H), 1.85 (m, 2 H), 0.99 (t, J = 7 Hz, 3 H). ^{13}C NMR (300 MHz, $CDCL_3$) δ 163.10, 151.86, 146.58, 140.34, 137.94, 137.00, 123.04, 117.01, 110.67, 54.53, 39.50, 32.60, 22.20, 16.27, 13.70.

Synthesis of 4-Alkylamino-imidazo[1,5-*a*]pyrido[3,2-*e*]pyrazines 22−24. General Procedure. First, 7 mmol of 4-chloro-imidazo[1,5-*a*]pyrido[3,2-*e*]pyrazine and 25 mL of an aqueous solution of methylamine or dimethylamine (40%) were stirred in an autoclave at 125−130 °C for 5 h. At room temperature, the mixture was extracted with 2 × 50 mL of dichloromethane. The organic solution was washed with 2 × 50 mL of water. The solvent was removed from the isolated organic layer. The residue was purified by column chromatography.

1-Ethyl-8-methoxy-3-methyl-4-methylamino-imidazo[1,5-*a*]-pyrido[3,2-*e*]pyrazine (22). Yield 88%; mp 172−174 °C; $C_{14}H_{17}N_5O$; MW 271.32. ^{1}H NMR (300 MHz, DMSO) δ 7.72 (d, J = 9 Hz, 1 H), 6.76 (d, J = 9 Hz, 1 H), 6.37 (q, J = 5 Hz, 1 H), 3.90 (s, 3 H), 3.46 (q, J = 8 Hz, 2 H), 2.94 (d, J = 5 Hz, 3 H), 2.56 (s, 3 H), 1.32 (t, J = 8 Hz, 3 H). ^{13}C NMR (300 MHz, DMSO) δ 157.20, 149.22, 144.89, 136.71, 134.12, 131.43, 126.96, 116.05, 108.54, 53.46, 28.00, 23.58, 15.12, 12.78.

8-Methoxy-3-methyl-4-methylamino-1-propyl-imidazo[1,5-*a*]-pyrido[3,2-*e*]pyrazine (23). See Supporting Information for details.

4-Dimethylamino-8-methoxy-3-methyl-1-propyl-imidazo[1,5-*a*]-pyrido[3,2-*e*]pyrazine (24). See Supporting Information for details.

Synthesis of 4-Cyano-imidazo[1,5-*a*]pyrido[3,2-*e*]pyrazines 25−27. General Procedure. First, 10 mmol of 4-chloro-imidazo-[1,5-*a*]pyrido[3,2-*e*]pyrazine were stirred into a solution of 32 g of ethoxycarbonyldifluoromethyl magnesia chloride in 100 mL of tetrahydrofuran. The mixture was stirred and heated up to reflux for 10 h. The solvent was removed. About 15 mL of *N*,*N*-dimethylformamide and 2 g of KCN were added. This reaction mixture was heated up to reflux for 5 h. After this time, 100 mL of toluene were added. After a stirring period of 10 min, the organic layer was separated and washed with 3 × 50 mL of water. The solvent was removed from the isolated organic layer. The residue was purified by column chromatography.

4-Cyano-8-methoxy-3-methyl-1-propyl-imidazo[1,5-*a*]pyrido-[3,2-*e*]pyrazine (25). Yield 70%; mp 178−180 °C; $C_{15}H_{15}N_5O$; MW 281.32. ^{1}H NMR (300 MHz, $CDCL_3$) δ 8.21 (d, J = 9 Hz, 1 H), 7.10 (d, J = 9 Hz, 1 H), 4.10 (s, 3 H), 3.86 (t, J = 8 Hz, 2 H), 2.02 (m, 2 H), 1.07 (t, J = 7 Hz, 3 H). ^{13}C NMR (300 MHz, $CDCL_3$) δ 164.33, 144.06, 141.72, 136.43, 130.17, 126.43, 126.38, 121.05, 113.98, 113.96 55.23, 30.13. 22.42, 13.61, 11.03.

4-Cyano-1-ethyl-8-methoxy-3-methyl-imidazo[1,5-*a*]pyrido-[3,2-*e*]pyrazine (26). See Supporting Information for details.

4-Cyano-1-cyclohexyl-8-methoxy-3-methyl-imidazo[1,5-*a*]pyrido-[3,2-*e*]pyrazine (27). See Supporting Information for details.

Synthesis of 4-Acetylamino- and 4-Propionylamino-imidazo-[1,5-*a*]pyrido[3,2-*e*]pyrazines 28−30. General Procedure. First, 30 mmol of 4-chloro-imidazo[1,5-*a*]pyrido[3,2-*e*]pyrazine and 200 mL of an aqueous solution of NH_3 (32%) were stirred in an autoclave at 125−130 °C for 8 h. The reaction mixture was diluted with 200 mL of water. The corresponding 4-amino-imidazo[1,5-a]pyrido[3,2-e]pyrazine precipitated. The crude intermediate was filtered off and washed with 50 mL of water. Finally, it was stirred with 30 mL of dichloromethane for 15 min at room temperature. After filtration, the intermediate was dried at room temperature.

First, 3 mmol of the corresponding 4-amino-imidazo[1,5-*a*]pyrido[3,2-*e*]pyrazine and 10 mL of acetic acid anhydride or propionic acid anhydride were stirred at 100 °C for 2 h. At room temperature, the mixture was diluted with 100 mL of ice−water. Solid sodium hydrogencarbonate is added until a pH value of 6.0 was achieved. The precipitated product was filtered off and washed with 50 mL of water. The product was purified by column chromatography.

4-Acetylamino-1-ethyl-8-methoxy-3-methyl-imidazo[1,5-*a*]pyrido-[3,2-*e*]pyrazine (28). Yield 90%; mp 199−202 °C; $C_{15}H_{17}N_5O_2$; MW 299.33. ^{1}H NMR (300 MHz, DMSO) δ 10.26 (s, 1 H), 8.01 (d, J = 9 Hz, 1 H), 6.95 (d, J = 9 Hz, 1 H), 3.99 (s, 3 H), 3.54 (q, J = 7 Hz, 2 H), 2.44 (s, 3 H), 2.13 (s, 3 H), 1.36 (t, J = 7 Hz, 3 H). ^{13}C NMR (300 MHz, DMSO) δ 170.44, 160.65, 145.40, 143.96, 139.28, 136.33, 134.49, 124.71, 119.83, 109.51, 54.01, 23.53, 23.03, 14.42, 12.82, 12.44.

4-Acetylamino-8-Methoxy-3-methyl-1-propyl-imidazo[1,5-*a*]-pyrido[3,2-*e*]pyrazine (29). See Supporting Information for details.

8-Methoxy-3-methyl-4-propionylamino-1-propyl-imidazo[1,5-*a*]pyrido[3,2-*e*]pyrazine (30). See Supporting Information for details.

Synthesis of 4-Alkoxycarbonylamino-imidazo[1,5-*a*]pyrido-[3,2-*e*]pyrazines 31−34. General Procedure. First, 30 mmol of 4-chloro-imidazo[1,5-*a*]pyrido[3,2-*e*]pyrazine and 200 mL of an aqueous solution of NH_3 (32%) were stirred in an autoclave at 125−130 °C for 8 h, then the reaction mixture was diluted with 200 mL of water. The corresponding 4-amino-imidazo[1,5-*a*]pyrido-[3,2-*e*]pyrazine precipitated. The crude intermediate was filtered off and washed with 50 mL of water. Finally, it was stirred with 30 mL of dichloromethane for 15 min at room temperature. After filtration, the intermediate was dried at room temperature.

First, 3 mmol of the corresponding 4-amino-imidazo[1,5-*a*]pyrido[3,2-*e*]pyrazine were stirred into a mixture of 20 mL of dichloromethane, 5 mL of methanol, and 1 mL of triethylamine. At 0 °C, a solution of 3 mmol of chloroformic acid ester in 10 mL of dichloromethane was added slowly. The reaction mixture was stirred for 2 h at 0 °C, then the solution was heated up to reflux for 10 h. At room temperature, the solution was washed with 30 mL of a saturated aqueous solution of sodium hydrogencarbonate and with 30 mL of water. The solvent was removed. The product was purified by column chromatography.

8-Methoxy-4-methoxycarbonylamino-3-methyl-1-propyl-imidazo-[1,5-*a*]pyrido[3,2-*e*]pyrazine (31). Yield 76%; mp 127−130 °C; $C_{16}H_{19}N_5O_3$; MW 329.36. ^{1}H NMR (300 MHz, DMSO) δ 9.88 (s, 1H), 8.00 (d, J = 9 Hz, 1 H), 6.94 (d, J = 9 Hz, 1 H), 3.98 (s, 3 H), 3.69 (s, 3 H), 3.49 (t, J = 8 Hz, 2 H), 2.46 (s, 3 H), 1.82 (m, 2 H), 0.97 (t, J = 7 Hz, 3 H). ^{13}C NMR (300 MHz, DMSO) δ 160.58, 154.73, 144.41, 143.33, 139.35, 136.24, 134.44, 124.77, 119.61, 109.62, 54.01, 52.22, 31.88, 21.40,14.45, 13.65.

4-Ethoxycarbonylamino-8-methoxy-3-methyl-1-propyl-imidazo-[1,5-*a*]pyrido[3,2-*e*]pyrazine (32). See Supporting Information for details.

4-(*N*,*N*-Bis-ethoxycarbonyl-amino)-8-methoxy-3-methyl-1-propyl-imidazo[1,5-*a*]pyrido[3,2-*e*]pyrazine (33). In this case, 6 mmol of chloroformic acid ethyl ester were used in the last step.

8-Methoxy-4-(methoxycarbonyl-methyl-amino)-3-methyl-1-propyl-imidazo[1,5-*a*]pyrido[3,2-*e*]pyrazine (34). 8-Methoxy-3-methyl-4-methylamino-1-propyl-imidazo[1,5-*a*]pyrido[3,2-*e*]-pyrazine (**23**) was used as the corresponding 4-amino-imidazo-[1,5-*a*]pyrido[3,2-*e*]pyrazine.

Synthesis of 4-Ureido-imidazo[1,5-*a*]pyrido[3,2-*e*]pyrazines 35−37. General Procedure. First, 30 mmol of 4-chloro-8-methoxy-3-methyl-1-propyl-imidazo[1,5-*a*]pyrido[3,2-*e*]pyrazine and 200 mL of an aqueous solution of NH_3 (32%) were stirred in an autoclave at 125−130 °C for 8 h, then the reaction mixture was diluted with 200 mL of water. The reaction product 4-amino-8-methoxy-3-methyl-1-propyl-imidazo[1,5-*a*]pyrido[3,2-*e*]pyrazine precipitated. The crude intermediate was filtered off and washed with 50 mL of water. Finally, it was stirred with 30 mL of dichloromethane for 15 min at room temperature. After filtration, the intermediate was dried at room temperature.

First, 2 mmol of 4-amino-8-methoxy-3-methyl-1-propyl-imidazo[1,5-*a*]pyrido[3,2-*e*]pyrazine were stirred into 20 mL of tetrahydrofuran at room temperature, then 6 mmol of carbonyldimidazole were added. The reaction mixture was heated up to reflux for 3 h. Then 20 mmol of NH_3 (aqueous solution, 32%) or methylamine (aqueous solution, 40%) or isopropylamine were added. Again, the mixture was heated up to reflux for 1 h. The solvent was removed. The residue was treated with 30 mL of water. The crude product precipitated. It was filtered off and washed with 50 mL of water. The product was purified by column chromatography.

8-Methoxy-3-methyl-1-propyl-4-ureido-imidazo[1,5-*a*]pyrido-[3,2-*e*]pyrazine (35). Yield 61%; mp 185−187 °C; $C_{15}H_{18}N_6O_2$; MW 314.35. ^{1}H NMR (300 MHz, $CDCL_3$) δ 9.35 (bs, 1 H), 7.73 (d, J = 9 Hz, 1 H), 7.22 (bs, 1 H), 6.77 (d, J = 9 Hz, 1 H), 5.63 (bs, 1 H), 3.99 (s, 3 H), 3.54 (t, J = 8 Hz, 2 H), 2.75 (s, 3 H), 1.88 (m, 2 H), 1.01 (t, J = 7 Hz, 3 H). ^{13}C NMR (300 MHz, $CDCL_3$) δ 160.28, 154.97, 146.22, 144.36, 137.58, 135.49, 132.88, 124.24, 115.56, 109.94, 54.14, 32.59, 22.15, 15.63, 13.84.

4-(*N*-Methyl-ureido)-8-methoxy-3-methyl-1-propyl-imidazo-[1,5-*a*]pyrido[3,2-*e*]pyrazine (36). See Supporting Information for details.

4-(*N*-Isopropyl-ureido)-8-methoxy-3-methyl-1-propyl-imidazo-[1,5-*a*]pyrido[3,2-*e*]pyrazine (37). See Supporting Information for details.

Synthesis of 4-Sulfonylamino-imidazo[1,5-*a*]pyrido[3,2-*e*]-pyrazines 38−45. General Procedure. First, 30 mmol of 4-chloro-imidazo[1,5-*a*]pyrido[3,2-*e*]pyrazine and 200 mL of an aqueous solution of NH_3 (32%) were stirred in an autoclave at 125−130 °C for 8 h, then the reaction mixture was diluted with 200 mL of water. The corresponding 4-amino-imidazo[1,5-*a*]pyrido[3,2-*e*]pyrazine precipitated. The crude intermediate was filtered off and washed with 50 mL of water. Finally, it was stirred with 30 mL of dichloromethane for 15 min at room temperature. After filtration, the intermediate was dried at room temperature.

A mixture of 30 mmol of the corresponding 4-amino-imidazo[1,5-*a*]pyrido[3,2-*e*]pyrazine with 50 mmol of an alkylsulfonic acid anhydride and 350 mL of toluol was heated up to reflux for 1 h. Then 15 mL triethylamine were added at about 70 °C. Again, the reaction mixture was stirred and heated to reflux for 1 h. The reaction mixture was treated with 100 mL of water. The precipitated crude product was filtered off and washed with 3 × 80 mL of water. The product was purified by recrystallization from toluol.

1-Ethyl-8-methoxy-3-methyl-4-methylsulfonylamino-imidazo-[1,5-*a*]pyrido[3,2-*e*]pyrazine (38). See Supporting Information for details.

8-Methoxy-3-methyl-4-methylsulfonylamino-1-propyl-imidazo-[1,5-*a*]pyrido[3,2-*e*]pyrazine (39). Yield 92%; mp 244−246 °C; $C_{15}H_{19}N_5O_3S$; MW 349.41. ^{1}H NMR (300 MHz, DMSO) δ 10.74 (s, 1 H), 8.16 (d, J = 9 Hz, 1 H), 6.80 (d, J = 9 Hz, 1 H), 3.87 (s, 3 H), 3.32 (t, J = 8 Hz, 2 H), 3.10 (s, 3 H), 2.54 (s, 3 H), 1.75 (m, 2 H), 0.94 (t, J = 7 Hz, 3 H). ^{13}C NMR (300 MHz, DMSO) δ 158.42, 146.76, 146.15, 142.59, 132.23, 130.47, 116.62, 108.55, 53.60, 42.22, 31.66, 20.60, 14.96, 13.21.

4-Ethylsulfonylamino-8-methoxy-3-methyl-1-propyl-imidazo-[1,5-*a*]pyrido[3,2-*e*]pyrazine (40). See Supporting Information for details.

8-Methoxy-3-methyl-4-propylsulfonylamino-1-propyl-imidazo-[1,5-*a*]pyrido[3,2-*e*]pyrazine (41). See Supporting Information for details.

4-Isopropylsulfonylamino-8-methoxy-3-methyl-1-propyl-imidazo-[1,5-*a*]pyrido[3,2-*e*]pyrazine (42). See Supporting Information for details.

4-(*N*,*N*-Bis-methylsulfonyl)-8-methoxy-3-methyl-1-propyl-imidazo[1,5-*a*]pyrido[3,2-*e*]pyrazine (43). In this case, 80 mmol of methylsulfonic acid anhydride were used in the last step.

8-Methoxy-3-methyl-1-propyl-4-trifluoromethylsulfonylamino-imidazo[1,5-*a*]pyrido[3,2-*e*]pyrazine (44). See Supporting Information for details.

8-Methoxy-3-methyl-4-(*N*-methylsulfonyl-*N*-methyl-amino)-1-propyl-imidazo[1,5-*a*]pyrido[3,2-*e*]pyrazine (45). 8-Methoxy-3-methyl-4-methylamino-1-propyl-imidazo[1,5-*a*]pyrido[3,2-*e*]pyrazine (**23**) was used as the corresponding 4-amino -imidazo-[1,5-*a*]pyrido[3,2-*e*]pyrazine.

8-Methoxy-3-methyl-1-propyl-imidazo[1,5-*a*]pyrido[3,2-*e*]-pyrazine (46). First, 3 mmol of 4-chloro-8-methoxy-3-methyl-1-propyl-imidazo[1,5-*a*]pyrido[3,2-*e*]pyrazine were suspended in 50 mL of ethanol, then about 1 mL of triethylamine and 1 g of palladium catalyst were added. This suspension was stirred in an autoclave. Hydrogen was pressed in up to 20 bar pressure. The mixture was stirred for 4 h at 30 °C. After filtration, the solvent was removed from the clear solution. The residue was dissolved in 100 mL of dichloromethane. The solution was washed with 50 mL of water. The solvent was removed again. The product was purified by column chromatography.

Yield 66%; mp 128−130 °C; $C_{14}H_{16}N_4O$; MW 256.31. ^{1}H NMR (300 MHz, DMSO) δ 8.78 (s, 1H), 8.10 (d, J = 9 Hz, 1 H), 6.96 (d, J = 9 Hz, 1 H), 3.99 (s, 3 H), 3.48 (t, J = 8 Hz, 2 H), 1.82 (m, 2 H), 0.97 (t, J = 7 Hz, 3 H). ^{13}C NMR (300 MHz, DMSO) δ 160.78, 143.81, 143.39, 140.23, 136.67, 134.38, 125.93, 123.17, 109.15, 54.01, 31.77, 21.44, 13.64, 12.35.

Synthesis of 4-Alkyl-imidazo[1,5-*a*]pyrido[3,2-*e*]pyrazines 47−59. General Procedure. First, 10 mmol of 4-chloro-imidazo[1,5-*a*]pyrido[3,2-*e*]pyrazine were suspended in 150 mL of tetrahydrofuran, then 30 mL of a solution of alkyl magnesium bromide in tetrahydrofuran (3M) were added. The mixture was stirred for 4 h at room temperature. After filtration, the solvent was removed from the clear solution. The product was purified by column chromatography.

8-Methoxy-1,3,4-trimethyl-imidazo[1,5-*a*]pyrido[3,2-*e*]pyrazine (47). See Supporting Information for details.

3,4-Dimethyl-1-ethyl-8-methoxy-imidazo[1,5-*a*]pyrido[3,2-*e*]-pyrazine (48). See Supporting Information for details.

3,4-Dimethyl-8-methoxy-1-propyl-imidazo[1,5-*a*]pyrido[3,2-*e*]-pyrazine (49). Yield 87%; mp 91−93 °C; $C_{15}H_{18}N_4O$; MW 270.33. ^{1}H NMR (300 MHz, $CDCL_3$) δ 7.87 (d, J = 9 Hz, 1 H), 6.73 (d, J = 9 Hz, 1 H), 3.96 (s, 3 H), 3.51 (t, J = 8 Hz, 2 H), 2.66 (s, 3 H), 2.65 (s, 3 H), 1.84 (m, 2 H), 0.98 (t, J = 7 Hz, 3 H). ^{13}C NMR (300 MHz, $CDCL_3$) δ 160.81, 152.32, 144.46, 139.11, 136.96, 134.63, 126.08, 123.14, 109.42, 54.02, 32.57, 23.57, 22.22, 15.76, 13.80.

8-Methoxy-4-methyl-1-propyl-imidazo[1,5-*a*]pyrido[3,2-*e*]pyrazine (50). See Supporting Information for details.

3,4-Dimethyl-1-propyl-imidazo[1,5-*a*]pyrido[3,2-*e*]pyrazine (51). See Supporting Information for details.

1-Propyl-3,4,8-trimethyl-imidazo[1,5-*a*]pyrido[3,2-*e*]pyrazine (52). See Supporting Information for details.

8-Difluoromethoxy-3,4-dimethyl-1-propyl-imidazo[1,5-*a*]pyrido-[3,2-*e*]pyrazine (53). See Supporting Information for details.

3,4-Dimethyl-8-methoxy-1-pentyl-imidazo[1,5-*a*]pyrido[3,2-*e*]-pyrazine (54). See Supporting Information for details.

1-Hexyl-8-methoxy-3,4-dimethyl-imidazo[1,5-*a*]pyrido[3,2-*e*]-pyrazine (55). See Supporting Information for details.

1-Cyclohexyl-3,4-dimethyl-8-methoxy-imidazo[1,5-*a*]pyrido-[3,2-*e*]pyrazine (56). See Supporting Information for details.

3,4-Dimethoxy-1-isobutyl-8-methoxy-imidazo[1,5-*a*]pyrido-[3,2-*e*]pyrazine (57). See Supporting Information for details.

1-Benzyl-3,4-dimethyl-8-methoxy-imidazo[1,5-*a*]pyrido[3,2-*e*]-pyrazine (58). See Supporting Information for details.

8-Methoxy-3,4-dimethyl-1-phenethyl-imidazo[1,5-*a*]pyrido-[3,2-*e*]pyrazine (59). See Supporting Information for details.

4-Difluoromethyl-8-methoxy-3-methyl-1-propyl-imidazo[1,5-*a*]-pyrido[3,2-*e*]pyrazine (60). To a solution of 100 mmol of 4-methyl-2-propyl-imidazole in 500 mL of dimethylformamide 120 mmol of KOH were added at 0 °C. The mixture was stirred for 10 min, then 100 mmol of 2-chloro-6-methoxy-3-nitropyridine were added to the mixture. The resulting solution was stirred at room temperature for 2 h. The solvent was removed under vacuum. The residue was diluted with water and extracted with 3 × 100 mL of ethyl acetate. The organic layer was washed with water and dried with magnesium sulfate. The solvent was evaporated under vacuum. The residue was purified by column chromatography to provide pure 6-methoxy-2-(4-methyl-2-propyl-imidazol-1-yl)-3-nitropyridine.

90 mmol of 6-methoxy-2-(4-methyl-2-propyl-imidazol-1-yl)-3-nitropyridine and 5 mmol of the palladium catalyst were stirred in 250 mL of tetrahydrofurane and 250 mL of methanol, then 500 mmol of ammonium formiate were added in small portions. This mixture was stirred at room temperature for 15 min and at 50 °C for 1 h. Filtration at room temperature yielded a clear solution. The solvent was removed. The reaction product 3-amino-6-methoxy-2-(4-methyl-2-propyl-imidazol-1-yl)-pyridine precipitated.

80 mmol of 3-amino-6-methoxy-2-(4-methyl-2-propyl-imidazol-1-yl)-pyridine was solved in 15 mL of acetic acid and 4 mL of difluoroacetic acid anhydride. The reaction mixture was stirred at room temperature for 1 h. A mixture of ice−water and ammonia was added. *N*-[6-Methoxy-2-(4-methyl-2-propyl-imidazol-1-yl)-pyridin-3-yl]-difluoroacetamide precipitated slowly. The product was filtered off and dried at 40 °C under vacuum.

50 mmol of *N*-[6-Methoxy-2-(4-methyl-2-propyl-imidazol-1-yl)-pyridin-3-yl]-difluoroacetamide were stirred in 30 mL of $POCL_3$, then 3 g of P_2O_5 were added. The reaction mixture was placed into an autoclave and heated up to 180 °C for 11 h, then it was pured into a mixture of ice−water and ammonia. The crude product precipitated. It was filtered off and purified by column chromatography.

Yield 88%; mp 114−117 °C; $C_{15}H_{16}F_2N_4O$; MW 306.31. ^{1}H NMR (300 MHz, DMSO) δ 8.19 (d, J = 9 Hz, 1 H), 7.10 (t, J = 54 Hz, 1 H), 7.02 (d, J = 9 Hz, 1 H), 4.01 (s, 3 H), 3.52 (t, J = 8 Hz, 2 H), 2.57 (s, 3 H), 1.83 (m, 2 H), 0.98 (t, J = 7 Hz, 3 H). ^{13}C NMR (300 MHz, DMSO) δ 162.08, 144.96, 144.64 (t, J = 27 Hz), 140.64, 137.10, 134.09, 123.99, 119.30, 114.09 (t, J = 244 Hz), 110.22, 54.30, 31.98, 21.32, 14.99, 13.61.

8-Methoxy-3-methyl-1-propyl-4-trifluoromethyl-imidazo[1,5-*a*]pyrido[3,2-*e*]pyrazine (61). First, 10 mmol of 4-chloro-8-methoxy-3-methyl-1-propyl-imidazo[1,5-*a*]pyrido[3,2-*e*]pyrazine and 15 mmol of HI (aqueous solution, 57%) were stirred at 0 °C for 3 h, then the reaction mixture was poured in 200 mL of an aqueous solution of $NaHCO_3$. To the stirred mixture, $Na_2S_2O_5$, 200 mL of water, and 200 mL of ethyl acetate were added. The organic layer was separated. The aqueous layer was washed twice with 50 mL of ethyl acetate. The combined organic layers were dried with $MgSO_4$. The solvent was removed by evaporation. The crude intermediate is used in the next step without further purification.

A mixture of 0.75 g KF and 2.5 g CuI was stirred and heated under vacuum until a homogeneous green color of the mixture was obtained. The reaction was cooled to room temperature, and the same procedure was done three times. After cooling to room temperature, 20 mL of NMP and 1.7 mL of $CF_3Si(CH_3)_3$ were added under nitrogen. The reaction mixture was stirred at 50 °C for 45 min. It was cooled to room temperature, and the previous prepared intermediate was added under nitrogen. The reaction mixture was stirred at 50 °C for 20 h. The mixture was cooled to room temperature, and aqueous ammonia was added. The organic layer was separated. The aqueous layer was washed three times with 10 mL of ethyl acetate. The combined organic layers were dried with $MgSO_4$. The solvent was removed by evaporation. The crude product was purified by column chromatography.

Yield 58%; mp 107−110 °C; $C_{15}H_{15}F_3N_4O$; MW 324.3. ^{1}H NMR (300 MHz, DMSO) δ 8.22 (d, J = 9 Hz, 1 H), 7.03 (d, J = 9 Hz, 1 H), 4.01 (s, 3 H), 3.51 (t, J = 8 Hz, 2 H), 2.51 (q, J = 1.5 Hz, 3 H), 1.83 (m, 2 H), 0.98 (t, J = 7 Hz, 3 H). ^{13}C NMR (300 MHz, DMSO) δ 162.64, 145.31, 140.95, 138.51 (q, J = 36 Hz), 137.33, 133.86, 132.22, 120.30 (q, J = 275 Hz), 118.30, 110.56, 54.44, 32.02, 21.23, 14.69 (q, J = 4 Hz), 13.60.

4-Ethyl-8-methoxy-3-methyl-1-propyl-imidazo[1,5-*a*]pyrido-[3,2-*e*]pyrazine (62). This compound was synthesized according to the general procedure for compounds **47**−**59** using ethyl magnesium bromide.

Yield 67%; mp 78−81 °C; $C_{16}H_{20}N_4O$; MW 284.36. ^{1}H NMR (300 MHz, $CDCL_3$) δ 7.85 (d, J = 9 Hz, 1 H), 6.68 (d, J = 9 Hz, 1 H), 3.92 (s, 3 H), 3.47 (t, J = 8 Hz, 2 H), 2.91 (q, J = 7 Hz, 2 H), 2.61 (s, 3 H), 1.81 (m, 2 H), 1.28 (t, J = 7 Hz, 3 H), 0.96 (t, J = 7 Hz, 3 H). ^{13}C NMR (300 MHz, $CDCL_3$) δ 160.67, 156.78, 144.37, 139.10, 136.75, 133.62, 126.04, 122.52, 109.24, 53.92, 32.59, 29.03, 22.15, 15.75, 13.76, 12.12.

8-Methoxy-3-methoxycarbonyl-4-methyl-1-propyl-imidazo-[1,5-*a*]pyrido[3,2-*e*]pyrazine (63). This compound was synthesized according to the procedure for compound **60**. 2-Propyl-imidazole-4-yl carboxylic acid methyl ester was used instead of 4-methyl-2-propyl-imidazole in the first step and acetic acid anhydride instead of difluoroacetic acid anhydride in the third step.

Yield 73%; mp 181−182 °C; $C_{16}H_{18}N_4O_3$; MW 314.34. ^{1}H NMR (300 MHz, DMSO) δ 8.22 (d, J = 9 Hz, 1 H), 7.10 (d, J = 9 Hz, 1 H), 4.04 (s, 3 H), 3.88 (s, 3 H), 3.61 (t, J = 8 Hz, 2 H), 2.84 (s, 3 H), 1.87 (m, 2 H), 1.00 (t, J = 7 Hz, 3 H).

3-Ethoxycarbonyl-8-methoxy-4-methyl-1-propyl-imidazo[1,5-*a*]pyrido[3,2-*e*]pyrazine (64). This compound was synthesized according to the procedure for compound **60**. 2-Propyl-imidazole-4-yl carboxylic acid ethyl ester was used instead of 4-methyl-2-propyl-imidazole in the first step and acetic acid anhydride instead of difluoroacetic acid anhydride in the third step.

Yield 71%; mp 158−159.5 °C; $C_{17}H_{20}N_4O_3$; MW 328.37. ^{1}H NMR (300 MHz, DMSO) δ 8.22 (d, J = 9 Hz, 1 H), 7.11 (d, J = 9 Hz, 1 H), 4.36 (q, J = 7 Hz, 2 H),4.04 (s, 3 H), 3.62 (t, J = 7 Hz, 2 H) 2.83 (s, 3 H), 1.87 (m, 2 H), 1.35 (t, J = 7 Hz, 3 H), 1.00 (t, J = 7 Hz, 3 H). ^{13}C NMR (300 MHz, DMSO) δ 160.19, 150.83, 144.78, 139.87, 135.34, 126.44, 125.72, 110.90, 60.58, 54.16, 32.29, 24.75, 21.22, 14.04, 13.49.

Screening. Inhibition of recombinant PDE10A (baculovirus/SF21 system). The DNA of PDE10A1 (AB 020593, 2340 bp) was synthesized and cloned into vector pCR4.TOPO (Entelechon GmbH, Regensburg, Germany). The gene was then inserted into a baculovirus vector, ligated with the baculovirus DNA, and the enzyme protein expressed in SF21 cells. To isolate the enzyme, cells were first harvested by centrifugation at 500 g followed by resuspension in 50 mM Tris-HCl/1 mM EDTA/250 mM sucrose buffer, pH = 7.4. (Sigma, Deisenhofen, Germany; Merck, Darmstadt, Germany) and lysis by sonication (3 × 15 s, Labsonic U, Fa. Braun, Degersheim, Switzerland, level setting "high"). Cytosolic PDE10A was obtained by centrifugation at 48000*g* for 1 h. The supernatant containing the active enzyme was stored at −70 °C.

PDE activity was determined applying a one-step procedure in microtiter plates. The reaction mixture contained 50 mM Tris-HCl/5 mM MgCl2 buffer (pH = 7.4. Sigma, Deisenhofen, Germany; Merck, Darmstadt, Germany), 0.1 μM [3H] cAMP (Amersham, Buckinghamshire, UK), and the enzyme in a total volume of 100 μL. Nonspecific activity was determined in the absence of enzyme. The reaction was initiated by addition of the substrate solution and carried out at 37 °C for 30 min. Enzymatic activity was stopped by addition of 25 μL Ysi-SPA-beads (Amersham-Pharmacia). After 1 h, the mixture was quantified

in a liquid scintillation counter for microtiter plates (Microbeta Trilux). Pipetting of the incubation mixture was routinely performed using the Biomek 2000 (Beckman). The optimal amount of enzyme to use per assay was determined for each enzyme preparation batch prior to usage in compound testing. IC_{50} values were determined using the Hill plot, two-parameter model.

MK-801-Induced Psychosis in Rats. Animals: Female Wistar rats (Crl: (WI) BR from Charles River, Germany) weighing 160−180 g were used. They were housed in groups of five under standard conditions on a 12 h light/dark cycle (lights on at 06:00 h) with ad libitum access to water and food (ssniff M/R 15, Spezialdiäten GmbH, Soest/Westfalen, Germany). Experiments were approved by the Committee for Animal Care and Usage of the Federal State of Saxony and carried out in accordance with German animal protection laws.

Experimental procedure: Behavior induced by the NMDA antagonist MK-801 is generally accepted as a rat model of psychosis. MK-801 induced stereotypies and hyperactivity in rats after intraperitoneal administration.[28]

Locomotor activity of the rats was recorded by the MotiTest apparatus (TSE, Bad Homburg, Germany). The test area consisted of a square arena (45 cm × 45 cm) with protective plexiglas walls (20 cm high) in which rats can move freely. Horizontal movements were recorded by 32 infrared photocells arranged along the bottom of each wall of the arena. The duration of activity was analyzed using the "ActiMot" computer program (TSE, Bad Homburg, Germany).

Stereotyped sniffing was scored by the experimenter every 5 min over a period of 1 h (12 intervals) according to the method described by Andiné et al.[28] The scores (0: no stereotyped sniffing; 1: discontinuous sniffing with free interval >5 s; 2: continuous sniffing) of the 12 intervals were added together for each parameter.

On the day of experimentation, rats receive the test compound or vehicle 30 min prior to test onset; 0.1 mg/kg MK-801 was administered intraperitoneally 10 min prior to testing. The rats were placed in the center of the square arena of the MotiTest apparatus 30 min before the start of the experiment to allow them to become accustomed to the environment. The behavior of the rats was then recorded for a period of 1 h.

Statistics: Results were analyzed by one way analysis of variance (ANOVA) when several groups were compared and by *t* test when two groups were compared. Tukey test was used for individual comparisons. $P < 0.05$ was regarded as significant.[31,32]

SAR Analysis. For the FWA, the negative base-10 logarithms of the IC_{50} (pIC_{50}) were used. In two cases (compounds **12**, **15**), only percent inhibition data *P* at inhibitor concentration [I] were available. Here, IC_{50E} values were estimated according to eq 1.[33]

$$IC_{50E} = [I] \times \frac{100 - P}{P} \quad (1)$$

The FWA matrix was compiled as described elsewhere[18] and evaluated with the SigmaStat program,[31] applying multiple linear regression analysis. Coefficients with probabilities >0.1 were considered to be not significantly different from zero, i.e., from the effect of a standard substitution at the respective position.

Docking. 3D structures of compounds **4**−**64** were generated from 2D sketches by means of Corina[34] and optimized by employing the semiempirical AM1 method[35] available within TSAR.[36] Docking into the binding pocket of PDE10A crystal structure 3LXG was carried out with program GOLD.[37] Mostly, default parameters and settings of GOLD were applied. The binding site was defined based on the position of **49** including residues within a radius of 18 Å. The number of docking runs was set to 30 for each compound and "early termination" was disabled. A water molecule known to play an essential role for binding of **49** (Figure 3) was retained. Calculations were biased toward solutions with a hydrogen bond to Gln716.

Acknowledgment. We thank Proteros Biostructures GmbH (Martinsried) for solving the crystal structure of the PDE10A/compound **49** complex. The presented investigations were funded by EFRE grants from the EU and by grants from the Free State of Saxony (project no. 12525).

Supporting Information Available: Analytical and spectroscopic results for compounds **4**−**64**, QSAR details, detailed pharmacological results, and X-ray crystallographic data. This material is available free of charge via the Internet at http://pubs.acs.org.

References

(1) Conti, M.; Beavo, J. Biochemistry and physiology of cyclic nucleotide phosphodiesterases: essential components in cyclic nucleotide signaling. *Annu. Rev. Biochem.* **2007**, *76*, 481–511.
(2) Bender, A. T.; Beavo, J. A. Cyclic nucleotide phosphodiesterases: molecular regulation to clinical use. *Pharmacol. Rev.* **2006**, *58*, 488–520.
(3) Essayan, D. M. Cyclic nucleotide phosphodiesterases. *J. Allergy Clin. Immunol.* **2001**, *108*, 671–680.
(4) Houslay, M. D.; Adams, D. R. PDE4 cAMP phosphodiesterases: modular enzymes that orchestrate signalling cross-talk, desensitization and compartmentalization. *Biochem. J.* **2003**, *370*, 1–18.
(5) Coskran, T. M.; Morton, D.; Menniti, F. S.; Adamowicz, W. O.; Kleiman, R. J.; Ryan, A. M.; Strick, C. A.; Schmidt, C. J.; Stephenson, D. T. Immunohistochemical localization of phosphodiesterase 10A in multiple mammalian species. *J. Histochem. Cytochem.* **2006**, *54*, 1205–1213.
(6) Seeger, T. F.; Bartlett, B.; Coskran, T. M.; Culp, J. S.; James, L. C.; Krull, D. L.; Lanfear, J.; Ryan, A. M.; Schmidt, C. J.; Strick, C. A.; Varghese, A. H.; Williams, R. D.; Wylie, P. G.; Menniti, F. S. Immunohistochemical localization of PDE10A in the rat brain. *Brain Res.* **2003**, *985*, 113–126.
(7) Xie, Z.; Adamowicz, W. O.; Eldred, W. D.; Jakowski, A. B.; Kleiman, R. J.; Morton, D. G.; Stephenson, D. T.; Strick, C. A.; Williams, R. D.; Menniti, F. S. Cellular and subcellular localization of PDE10A, a striatum-enriched phosphodiesterase. *Neuroscience* **2006**, *139*, 597–607.
(8) Lapiz, M. D.; Fulford, A.; Muchimapura, S.; Mason, R.; Parker, T.; Marsden, C. A. Influence of postweaning social isolation in the rat on brain development, conditioned behavior, and neurotransmission. *Neurosci. Behav. Physiol.* **2003**, *33*, 13–29.
(9) Siuciak, J. A.; McCarthy, S. A.; Chapin, D. S.; Fujiwara, R. A.; James, L. C.; Williams, R. D.; Stock, J. L.; McNeish, J. D.; Strick, C. A.; Menniti, F. S.; Schmidt, C. J. Genetic deletion of the striatum-enriched phosphodiesterase PDE10A: evidence for altered striatal function. *Neuropharmacology* **2006**, *51*, 374–385.
(10) Siuciak, J. A.; Chapin, D. S.; Harms, J. F.; Lebel, L. A.; McCarthy, S. A.; Chambers, L.; Shrikhande, A.; Wong, S.; Menniti, F. S.; Schmidt, C. J. Inhibition of the striatum-enriched phosphodiesterase PDE10A: a novel approach to the treatment of psychosis. *Neuropharmacology* **2006**, *51*, 386–396.
(11) Kostowski, W.; Gajewska, S.; Bidzinski, A.; Hauptman, M. Papaverine, drug-induced stereotypy and catalepsy and biogenic amines in the brain of the rat. *Pharmacol., Biochem. Behav.* **1976**, *5*, 15–17.
(12) Rodefer, J. S.; Murphy, E. R.; Baxter, M. G. PDE10A inhibition reverses subchronic PCP-induced deficits in attentional set-shifting in rats. *Eur. J. Neurosci.* **2005**, *21*, 1070–1076.
(13) Pandit, J. Crystal structure of 3′,5′-cyclic nucleotide phosphodiesterase (PDE10A) and uses thereof. U.S. Patent 2005/0202550 A1, 2005.
(14) Siuciak, J. A., Chapin, D. S., McCarthy, S. A., Harms, J. F., Fox, C. B., Chappie, T. A., Humphrey, J. M., Proulz, C., Verhoest, P. R., Schmidt, C. J. Novel potent and selective phosphodiesterase 10A (PDE10A) inhibitors show activity in animal models of psychosis. Society for Neuroscience Annual Meeting, Atlanta, GA, 2006.
(15) Chappie, T.; Humphrey, J.; Menniti, F.; Schmidt, C. PDE10A inhibitors: an assessment of the current CNS drug discovery landscape. *Curr. Opin. Drug Discovery Dev.* **2009**, *12*, 458–467.
(16) Kehler, J.; Ritzen, A.; Greve, D. R. The potential therapeutic use of phosphodiesterase 10 inhibitors. *Expert. Opin. Ther. Patents* **2007**, *17*, 147–158.
(17) Norris, D.; Chen, P.; Barrish, J. C.; Das, J.; Moquin, R.; Chen, B.-C.; Guo, P. Synthesis of imidazo[1,5-*a*]quinoxalin-4(5*H*)-one template via a novel intramolecular cyclization process. *Tetrahedron Lett.* **2001**, *42*, 4297–4299.

(18) Free, S. M., Jr.; Wilson, J. W. A mathematical contribution to structure−activity studies. *J. Med. Chem.* **1964**, *53*, 395–399.
(19) Fujita, T.; Ban, T. Structure−activity study of phenethylamines as substrates of biosynthetic enzymes of sympathetic transmitters. *J. Med. Chem.* **1971**, *14*, 148–152.
(20) Benigni,R.; Giuliani,A.; Gruska,A.; and Franke,R. Introductory discussion on QSAR. In *Quantitative Structure−Activity Relationship (QSAR) Models of Mutagens and Carcinogens*; Benigni, R., Ed.; CRC Press: Boca Raton, FL, 2003; pp 1−38.
(21) Chappie, T. A.; Humphrey, J. M.; Allen, M. P.; Estep, K. G.; Fox, C. B.; Lebel, L. A.; Liras, S.; Marr, E. S.; Menniti, F. S.; Pandit, J.; Schmidt, C. J.; Tu, M.; Williams, R. D.; Yang, F. V. Discovery of a series of 6,7-dimethoxy-4-pyrrolidylquinazoline PDE10A inhibitors. *J. Med. Chem.* **2007**, *50*, 182–185.
(22) Huai, Q.; Wang, H.; Sun, Y.; Kim, H. Y.; Liu, Y.; Ke, H. Three-dimensional structures of PDE4D in complex with roliprams and implication on inhibitor selectivity. *Structure* **2003**, *11*, 865–873.
(23) Andersen, O. A.; Schonfeld, D. L.; Toogood-Johnson, I.; Felicetti, B.; Albrecht, C.; Fryatt, T.; Whittaker, M.; Hallett, D.; Barker, J. Cross-linking of protein crystals as an aid in the generation of binary protein−ligand crystal complexes, exemplified by the human PDE10a-papaverine structure. *Acta Crystallogr., Sect. D: Biol. Crystallogr.* **2009**, *65*, 872–874.
(24) Conti, M. A view into the catalytic pocket of cyclic nucleotide phosphodiesterases. *Nat. Struct. Mol. Biol.* **2004**, *11*, 809–810.
(25) Ke, H.; Wang, H. Crystal structures of phosphodiesterases and implications on substrate specificity and inhibitor selectivity. *Curr. Top. Med. Chem.* **2007**, *7*, 391–403.
(26) Verhoest, P. R.; Chapin, D. S.; Corman, M.; Fonseca, K.; Harms, J. F.; Hou, X.; Marr, E. S.; Menniti, F. S.; Nelson, F.; O'Connor, R.; Pandit, J.; Proulx-LaFrance, C.; Schmidt, A. W.; Schmidt, C. J.; Suiciak, J. A.; Liras, S. Discovery of a Novel Class of Phosphodiesterase 10A Inhibitors and Identification of Clinical Candidate 2-[4-(1-Methyl-4-pyridin-4-yl-1*H*-pyrazol-3-yl)-phenoxymethyl]-quinoline (PF-2545920) for the Treatment of Schizophrenia. *J. Med. Chem.* **2009**, *52*, 5188–5196.
(27) Zhang, K. Y.; Card, G. L.; Suzuki, Y.; Artis, D. R.; Fong, D.; Gillette, S.; Hsieh, D.; Neiman, J.; West, B. L.; Zhang, C.; Milburn, M. V.; Kim, S. H.; Schlessinger, J.; Bollag, G. A glutamine switch mechanism for nucleotide selectivity by phosphodiesterases. *Mol. Cell* **2004**, *15*, 279–286.
(28) Andiné, P.; Widermark, N.; Axelsson, R.; Nyberg, G.; Olofsson, U.; Martensson, E. and Sandberg, M. Characterization of MK-801-induced behavior as a putative rat model of psychosis. *J. Pharmacol. Exp. Ther.* **1999**, *290*, 1393–1408.
(29) Capuano, B.; Crosby, I. T.; Lloyd, E. J. Schizophrenia: genesis, receptorology and current therapeutics. *Curr. Med. Chem.* **2002**, *9*, 521–548.
(30) Chen, P., Norris, D. J., Barrish, J. C., Iwanowicz, E. J., Gu, H. H., Schieven, G. L. Heterocyclo-substituted imidazopyrazine protein tyrosine kinase inhibitors. Patent WO/1999/045009, 1998
(31) *SigmaStat, version 3.11*; Systat Software, Inc.: Chicago, **2004**.
(32) *SigmaPlot 2004, version 9.0*; Systat Software, Inc.: Chicago, **2004**.
(33) Grunwald, C.; Rundfeldt, C.; Lankau, H. J.; Arnold, T.; Höfgen, N.; Dost, R.; Egerland, U.; Hofmann, H. J.; Unverferth, K. Synthesis, Pharmacology, and Structure−Activity Relationships of Novel Imidazolones and Pyrrolones as Modulators of GABA-(A) Receptors. *J. Med. Chem.* **2006**, *49*, 1855–1866.
(34) *Corina, version 1.82*; Oxford Molecular Group: The Medawar Centre, Oxford Science Park, Oxford OX4 4GA, UK, **2000**.
(35) Clark, T., Alex, A., Beck, B., Chandrasekhar, J., Gedeck, P., Horn, A., Hutter, M., Martin, B., Rauhut, G., Sauer, W., Schindler, T., Steinke, T. *VAMP, version 7.5a*; The Oxford Molecular Group: The Medawar Centre, Oxford Science Park, Oxford OX4 4GA, UK, **1999**.
(36) *TSAR 3D, version 3.3*; Oxford Molecular Ltd (now Accelrys): The Medawar Centre, Oxford Science Park, Oxford OX4 4GA, UK, **2000**.
(37) *GOLD, version 4.1.2*; CCDC Software Ltd.: Cambridge, UK, **2010**.
(38) Wallace, A. C.; Laskowski, R. A.; Thornton, J. M. LIGPLOT: a program to generate schematic diagrams of protein−ligand interactions. *Protein Eng.* **1995**, *8*, 127–134.